

# Two-pulse structured illumination imaging

Elias Kristensson,\* Edouard Berrocal, and Marcus Aldén

*Division of Combustion Physics, Lund University, Sweden*

*\*Corresponding author: elias.kristensson@forbrf.lth.se*

Received January 24, 2014; revised March 21, 2014; accepted March 22, 2014;  
posted March 24, 2014 (Doc. ID 205468); published April 18, 2014

Structured illumination (SI), which is an imaging technique that is employed in a variety of fields, permits unique possibilities to suppress unwanted signal contributions that carry misleading information such as out-of-focus light or multiply scattered light. So far SI has been applied mostly for averaged imaging or for imaging of slowly occurring events because it requires three acquisitions (subimages) to construct the final SI image. This prerequisite puts technological constraints on SI that make “instantaneous” imaging of fast transient processes (occurring on sub-microsecond time scales) very challenging and expensive. Operating SI with fewer subimages generates errors in the form of residual lines that stretch across the image. Here, a new approach that circumvents this limiting factor is presented and experimentally demonstrated. By judiciously choosing the intensity modulation, it is possible to extract an SI image from two subimages only. This development will allow standard double-pulsed lasers and interline transfer CCD or scientific CMOS cameras to be used to acquire temporally frozen SI images of rapidly occurring processes as well as to boost the frame-rate of current SI video systems; a technical advancement that will benefit both macro- and microscopic imaging applications. © 2014 Optical Society of America

*OCIS codes:* (110.0180) Microscopy; (120.4820) Optical systems; (290.4210) Multiple scattering; (220.2945) Illumination design.

<http://dx.doi.org/10.1364/OL.39.002584>

With its ability to both perform optical sectioning and attain super-resolution images, structured illumination (SI) has become a vital tool within microscopic imaging [1–4]. However, SI has also spread into other research fields, and it can, for example, be employed to determine the topography of a sample [5], perform 3-D tomographic reconstructions [6], image underwater [7], and visualize atomizing spray systems for combustion purposes [8]. Regardless of the application, the basic principle of SI is to form a periodic line illumination pattern, either by projecting a grid or interfering two coherent beams, and to guide this spatially modulated illumination field onto the sample. The purpose of this rather unique illumination scheme is manifold and depends on the application; in microscopy, the fringe pattern marks the in-focus plane; in spray visualization, it serves as means to distinguish between singly and multiply scattered light; in shape determination, the deformation of the projected pattern reveals the topography of the sample. However, even though different applications incorporate SI for different reasons they all rely on a demodulation scheme, the most common being the phase-shifting method [1–9]. In this method, three acquisitions ( $I_0$ ,  $I_{120}$ , and  $I_{240}$ ), often referred to as *subimages*, are recorded between which the spatial phase of the superimposed fringe pattern is shifted  $120^\circ$ . The RMS of these subimages is then extracted, a mathematical operation that has two purposes. First, it removes all sub-image components that are identical whereas unique image features remain. This is the primary purpose of SI. Second, it removes the spatial modulation.

Unavoidably, multiple recordings render longer acquisition times. For averaged imaging this is mostly considered a matter of inconvenience, yet for instantaneous imaging of rapid events, this requirement becomes a limiting factor. Attaining a “single-shot” (temporally frozen) SI image of a transient phenomenon that occurs on a submicrosecond time scale requires a very complicated optical arrangement comprising three individual

pulsed lasers and three microchannel plate (MCP)-equipped cameras (to avoid cross talk between the laser pulses), as demonstrated by Kristensson *et al.* [9]. The cost of this approach thus greatly exceeds that of the averaged scheme, which only requires a single camera and a single (continuous or pulsed) light source.

The prerequisite for *three* subimages is particularly unfortunate; a setup based on *two* subimages would yield a considerable reduction of both the overall cost and complexity for high-speed applications as this would allow standard double-pulsed lasers and interline transfer CCDs or sCMOS cameras to be used. In addition, such a setup would open doors for high-speed imaging and particle image velocimetry applications using SI.

In an attempt to circumvent the issue with multiple acquisitions, Krzewina and Kim [10] demonstrated an SI setup consisting of white light LED illumination together with a color grid pattern to record all three subimages simultaneously using a color sensitive camera. However, this arrangement, in which the subimages are spectrally separated, should only be employed when reflected light is studied, as refraction and scattering (both elastic and inelastic) may be highly wavelength dependent. Wicker and Heintzmann [11] also presented a setup capable of instantaneous SI imaging. Instead of using different colors, the authors demonstrated the possibility to code the SI subimages differently by means of a sophisticated polarization scheme. The approach is, however, restricted to samples with polarization-maintaining properties. In 2008, Lim *et al.* [12] demonstrated an original imaging technique (called HiLo) capable of optical sectioning based only on two recordings using both homogeneous and speckle illumination. These recordings are then computationally combined to generate the final image. Despite its merits and ability to perform optical sectioning, HiLo differs from SI on many aspects and, for example, cannot be combined with side-scattering detection, nor does it allow spatial lock-in analysis [13].

In this Letter, a general approach to extract an SI image from only two subimages is presented and its suitability for “instantaneous” imaging is experimentally demonstrated on an atomizing water spray system using a planar SI approach. We call the approach two-pulse SI.

The idea of two-pulse SI is to illuminate the sample with two phase-mismatched intensity modulated laser beams (or, in this case, sheets) successively and to extract the absolute value of the intensity difference between these two subimages according to  $|I_0 - I_{180}|$  (by mismatching the spatial phases, the fringe overlap is minimized). This will remove the image components that are identical in the subimages, which is similar to the standard three-pulse SI approach. However, even though this approach would, in theory, suppress out-of-focus contributions, multiply scattered light, or similar unwanted image elements, the problem lies in the demodulation of the fringes; it is not possible to accurately reconstruct an SI image from two subimages only. The lack of information originally carried by the third, currently missing subimage will lead to an incomplete demodulation, where traces of the incident line structure will remain and distort the final SI image. Similar traces, commonly referred to as *residuals*, can also be observed in standard SI as well, e.g., when the grating is inaccurately shifted or when the illumination source undergoes large temporal variations [14]. The negative impact of these residuals often outweighs the improvement realized by SI, which explains why the two-pulse approach has been avoided in the past. However, there is a solution to either mitigate or, in the best case, completely avoid these errors thus making the two-pulse approach feasible.

To understand the solution, it is useful to think of each subimage in reciprocal space (i.e., its Fourier transform), wherein each element represents a certain spatial frequency component  $\nu$ . Image structures with low spatial frequencies reside close to the origin while high-resolution information resides further away. The highest resolvable frequencies ( $\nu_{\max}$ ) in a given image form a circular region around the origin; no finer image details can be observed beyond this so-called observable region [3]. Note that the position of this border is not always dictated by the pixel density of the camera but is also influenced by the camera objective, solid angle of collection, various amplification stages, etc. It may also depend on the sample itself, which is especially true for spray visualization where the probed sample inherently acts as a low-pass (smoothing) filter. It is, for these reasons, convenient to normalize the observable frequencies with respect to the highest spatial frequency component. With that representation, the highest resolvable feature ( $\bar{\nu}_{\max}$ ) of an imaging system equals unity, regardless of the number of pixels.

The Fourier transform of an SI subimage contains three prominent points: the dc-offset and the fundamental frequency component—ground-frequency—of the sinus-striped illumination, which appears symmetrically around the central dc point. This is illustrated in Fig. 1 for two sinusoidal frequencies that are superimposed on a flat intensity field. Each example is accompanied by its corresponding two-pulse SI image (to the right), i.e., constructed from two phase-mismatched subimages. As mentioned previously, the apparent stripy residual

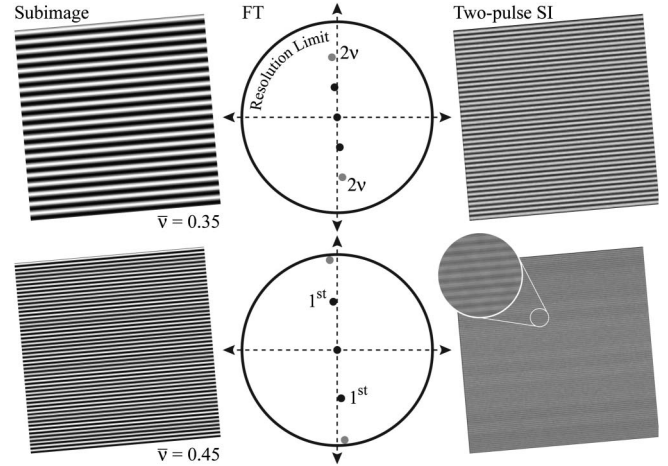


Fig. 1. Two-pulse SI (right column) generates residual lines ( $2\nu$ ) with a spatial frequency twice that of the ground-frequency. Thus, by increasing the ground-frequency,  $1^{st}$ , of the subimages (left column) the residuals become less apparent, and eventually, they reside at the border of the observable region where they are nearly indistinguishable. FT, Fourier transform.

line structures are caused by a lack of information that ordinarily is provided by the third subimage. Note that these residuals are always formed in a two-pulse SI scheme. However, two important features can be observed in the two-pulse SI images. First, the fundamental frequency of the residual lines is exactly twice that of their corresponding ground-frequency. Second, the undesired residuals become less pronounced as the ground-frequency increases. The explanation for this lies in the Fourier transform of each image: as the ground-frequency increases, the residuals are forced toward the border of the observable region and eventually, as the ground-frequency approaches  $\bar{\nu} = 0.5$ , they are close to indistinguishable and hardly distort the image. If the resolution of the detector is dictated by collection optics and not pixel density, the ground-frequency could be increased beyond this point, thus making the residuals so fine that the imaging system, in practice, “fails” to resolve them. In this way it is possible to extract a two-pulse SI image, completely free from residuals. However, for a pixel-limited system, increasing the ground-frequency beyond  $\bar{\nu} = 0.5$  will not lead to a more favorable situation as the residuals will be aliased at a lower spatial frequency. The effect is explained by the Nyquist theorem, which states that an under-sampled signal will appear at a lower frequency than its true value. In this situation, it is advised to select  $\bar{\nu} = 0.5$  and to reject the remaining traces of the spatial modulation by means of a low-pass filter. With the residuals appearing around  $\bar{\nu} = 1.0$ , the cutoff frequency ( $f_c$ ) of the low-pass filter can be chosen so that it hardly influences the image quality. This approach thus also allows the extraction of a residual-free two-pulse SI image, but at the cost of spatial resolution.

Figure 2 shows an example of two-pulse planar SI imaging (ensemble-averaged) applied on a hollow-cone water spray operating at a pressure of 20 bars. The setup employed in the example falls within the second category, i.e., limited by the number of pixels and relies therefore on low-pass filtering in order to avoid residual

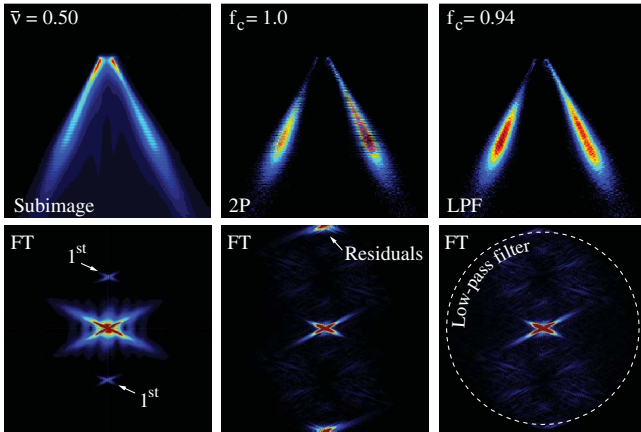


Fig. 2. Example of a two-pulse (2P) SI image in which the ground-frequency is  $\bar{\nu} = 0.50$ , thus generating residuals exactly at the resolution limit. These unwanted fringes are easily removed by means of a low-pass filter (LPF), which, because of the carefully chosen ground-frequency, hardly affects the image quality.  $f_c$  is the cutoff frequency.

line structures. However, with the carefully chosen ground-frequency ( $\bar{\nu} = 0.50$ ), the residuals fall exactly on the resolution limit and nearly no spatial resolution has to be sacrificed in the filtering process. If low spatial frequencies are the main interest, the ground-frequency can be reduced, which improves the signal-to-noise ratio and sometimes simplifies the experimental setup.

Two important aspects of the proposed two-pulse SI approach that need to be investigated are accuracy and precision. In this proof-of-concept study, these factors were studied on ensemble-averaged data by comparing the results with other results obtained using the standard (three-pulse) SI method, where no spatial resolution is sacrificed. In the comparison, the near nozzle region of the hollow-cone spray was probed with gradually increasing ground-frequencies; the results are shown in Fig. 3. Note that changing the ground-frequency required realignment and the spray may for this reason appear different for the different measurements. The study revealed that relatively low ground-frequencies provide unsatisfactory results. For example, the thickness of the liquid sheet at the nozzle exit was overestimated in the two low-frequency cases, as seen in the insets. The cross sections also highlight deviations seen in these images, e.g., the inner hollow region is inaccurately depicted in these cases. However, the results also show that selecting a sufficiently high ground-frequency (in this case  $\bar{\nu} > 0.20$ ) leads to negligible differences between the two- and three-pulse SI approaches ( $R^2 > 0.98$ ). This implies that this particular spray structure is primarily described by spatial frequencies below  $\bar{\nu} \approx 0.45$  and that rejecting higher frequencies has very little effect on the end result. As explained above, a ground-frequency of  $\bar{\nu} = 0.50$  would yield the least loss of spatial resolution, yet these test cases illustrate that there is not always a need to select such a high ground-frequency. Although, because SI is employed in so many different fields, it is advised, for each application, to investigate and determine the spatial frequencies deemed necessary to resolve those sample details of interest. Since the

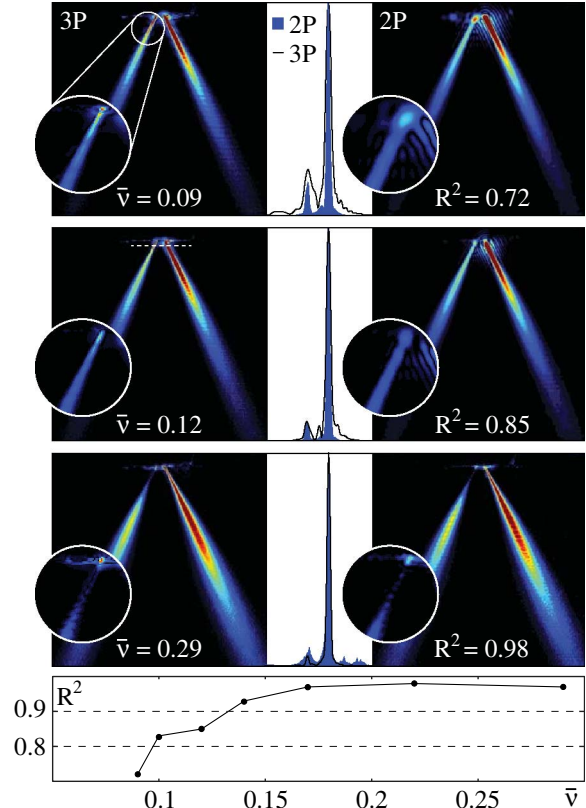


Fig. 3. Comparison between two- and three-pulse (3P) planar SI (ensemble-averaged). The investigation shows that, for this particular sample, a too low ground-frequency leads to significant deviations between the two approaches. The similarity (coefficient of determination,  $R^2$ ) between the 2P and 3P images was calculated over the entire image. Besides each example, a cross section (indicated by the dashed line) is provided. Also included is a plot showing how the value of  $R^2$  changes as a function of  $\bar{\nu}$  for the current sample.

signal-to-noise ratio in the SI image reduces with increasing ground-frequency, it is beneficial to select the lowest possible ground-frequency.

As mentioned above, the main motivation for the current work was to reduce the experimental complexity associated with “single-shot” imaging by means of SI. Examples of such images are presented in Fig. 4, and these show the region near the nozzle of the hollow-cone spray. The two-pulse planar SI images were sequentially acquired using two individual pulsed Nd:YAG lasers (10 ns pulse length) in combination with an sCMOS (LaVision, Imager), which allowed a pulse separation of 150 ns. In an ideal case, the injected liquid remains static during this time interval, as all detectable movements lead to errors in the data processing. The two laser pulses first passed a grating (phase-mismatched from each other) and were thereafter spatially overlapped using a 50:50 beam splitter, see diagram in Fig. 4. Despite being low-pass filtered ( $f_c = 0.45$ ), the SI images present improvements in both image contrast and fidelity, revealing structural features that are important for spray characterization. The “off-axis illumination” shows the shape of the spray in a region behind the central axis where the signal from multiple light scattering is evident, especially below the nozzle tip where no signal

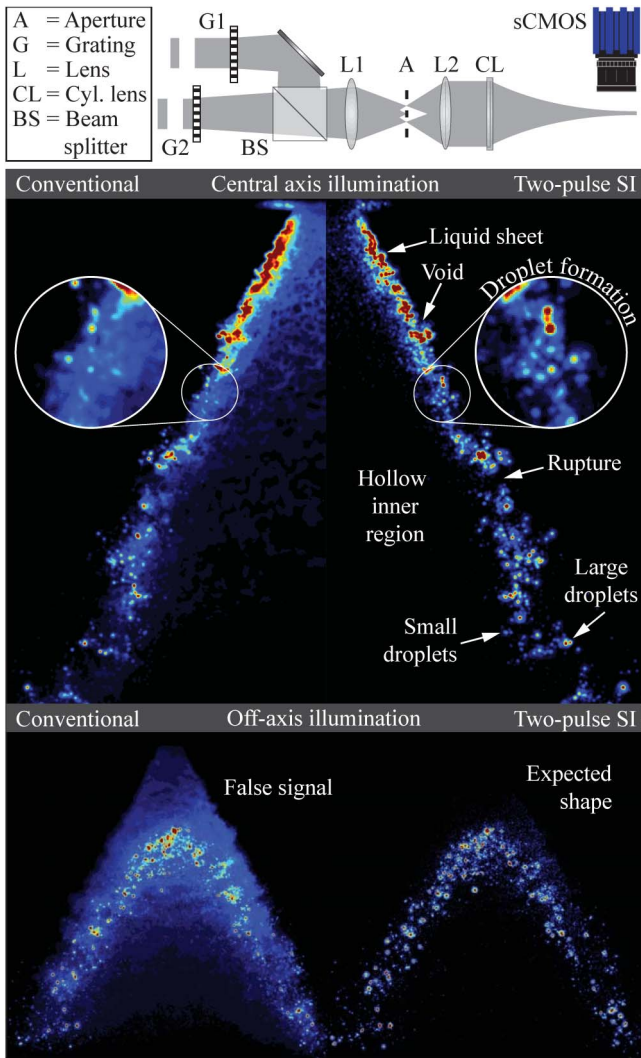


Fig. 4. Comparison between single-shot conventional laser sheet imaging and instantaneous two-pulse planar SI imaging together with a schematic of the optical arrangement. A low-pass filter with a cutoff frequency of  $f_c = 0.45$  was applied on the SI images, yet the loss of high spatial frequencies did not cause any evident distortion. On the contrary, finer details and sharper image gradients were observed in the SI cases thanks to the removal of the blur caused by multiply scattered photons. In the “off-axis” case, where a region behind the central axis of the hollow-cone spray was probed, the conventional laser sheet image clearly shows a signal in regions that were not directly illuminated. In contrast, with the two-pulse SI approach, the expected arc-like shape of the spray was restored.

is expected. Notice how the expected arc-like shape of the spray in this off-axis region is restored when employing two-pulse SI.

In conclusion, an SI setup based on two subimages has been developed and experimentally demonstrated, both for averaged and “instantaneous” imaging. By judiciously

selecting the ground-frequency of the SI fringe pattern, the residual line structures—unavoidably generated in the two-pulse process—can be strategically placed (in reciprocal space) so that they either become completely indistinguishable or have a nearly insignificant effect on the end result. The primary benefit of the presented approach is a significant reduction of the experimental complexity for high-speed applications, where close to instantaneous realizations are essential. Acquiring such temporally frozen data have previously required three individual pulsed lasers and MCP-gated cameras—with this new method similar results could be obtained using a single (double-pulsed) laser in combination with an interline transfer CCD or sCMOS, i.e., standard Particle Image Velocimetry (PIV) laboratory equipment. Such improvements will, however, not only benefit high-speed applications, currently available SI instruments could take advantage of this advancement as well.

Finally, the authors wish to thank the Linné Center within the Lund Laser Center as well as the Centre for Combustion Science and Technology through the Swedish Energy Agency for financial support. Also, the European Research Council Advanced Grant *Development and Application of Laser Diagnostic Techniques for Combustion Studies* and the foundation of Walter Gyllenberg are acknowledged.

## References

1. M. A. A. Neil, R. Juškaitis, and T. Wilson, *Opt. Lett.* **22**, 1905 (1997).
2. D. S. Elson, J. Siegel, S. E. D. Webb, S. Lévêque-Fort, D. Parsons-Karavassilis, M. J. Cole, P. M. W. French, D. M. Davis, M. J. Lever, R. Juškaitis, M. A. A. Neil, L. O. Sucharov, and T. Wilson, *J. Mod. Opt.* **49**, 985 (2002).
3. M. Gustafsson, *J. Microsc.* **198**, 82 (2000).
4. A. Jost and R. Heintzmann, *Annu. Rev. Mater. Res.* **43**, 261 (2013).
5. B. A. Rajoub, D. R. Burton, and M. J. Lalor, *J. Opt. A* **7**, S368 (2005).
6. D. J. Cuccia, F. Bevilacqua, A. J. Durkin, and B. J. Tromberg, *Opt. Lett.* **30**, 1354 (2005).
7. F. Bruno, G. Bianco, M. Muzzupappa, S. Barone, and A. V. Rationale, *ISPRS J. Photogr. Remote Sens.* **66**, 508 (2011).
8. E. Berrocal, E. Kristensson, M. Richter, M. Linne, and M. Aldén, *Opt. Express* **16**, 17870 (2008).
9. E. Kristensson, E. Berrocal, M. Richter, and M. Aldén, *Atomiz. Spr.* **20**, 337 (2010).
10. L. G. Krzewina and M. K. Kim, *Opt. Lett.* **31**, 477 (2006).
11. K. Wicker and R. Heintzmann, *J. Opt.* **12**, 084010 (2010).
12. D. Lim, K. K. Chu, and J. Mertz, *Opt. Lett.* **33**, 1819 (2008).
13. E. Kristensson, J. Bood, M. Aldén, E. Nordström, J. Zhu, S. Hultdt, P. E. Bengtsson, H. Nilsson, E. Berrocal, and A. Ehn, *Opt. Express* **22**, 7711 (2014).
14. L. H. Schaefer, D. Schuster, and J. Schaffer, *J. Microsc.* **216**, 165 (2004).